Earthquake Engineering, Tenth World Conference © 1992 Balkema, Rotterdam. ISBN 90 5410 060 5

A practical method of obtaining dynamic interaction of soil and embedded cylindrical structure in consideration of its backfill effects

Y.Shimomura
Nihon University, Japan
Y.Ikeda & H.Tajimi
Tajimi Engineering Services Ltd, Japan

ABSTRACT: The paper proposes a method of obtaining the interaction stiffnesses of a foundation embedded in the radially inhomogeneous soil and undergoing sway-rocking motion. The analysis model is constructed by (1) discretizing the soil stratum into a number of thin layers, (2) obtaining the laterally axial, shear and rotational stiffnesses of a circular rigid plate embedded in a layer which consists of annular inner and outer zones, and (3) distributing the stiffnesses along the embedment depth in accordance with the soil property variation and at the same time considering the modification of shear stiffness due to the series connection. The method is verified by the simulation analysis performed to the experimental test of the forced vibration tests of a reinforced concrete block.

1 INTRODUCTION

The rigidity of soil surrounding and neighboring an embedded structure is frequently reduced due to excavation and backfill works. Among the analyses discussed such reduction, two studies by Novak et al. (1980) and Veletsos et al. (1988) are well known. The former disregarded the mass of the soil close to the structure, while the latter took this effect into consideration. The present analysis follows the latter and introduces the shear stiffness to evaluate positively the soil reaction which probably transmits downward to the hard soil other than toward horizontally. The method treats a circular foundation undergoing sway-rocking motion and proceeds (1) to discretize the soil stratum into a number of thin layers, (2) to take a single layer into account to obtain the laterally axial, shear and rotational stiffnesses of a circular rigid plate embedded in the layer which consists of annular inner and outer zones, and (3) to construct the sway-rocking model by distributing the above stiffnesses for single layer along the embedment depth in accordance with the soil property variation and modifying the shear stiffness owing to the series connection, as shown in Fig. 1. To verify the effectiveness of the proposed method, a simulation analysis is performed and discussed by the results of the forced vibration test of the reinforced concrete block (Mizuno et al., 1985).

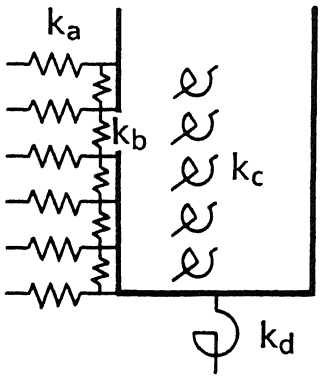

Figure 1. Soil spring model for an embedded structure.

2 STIFFNESS FUNCTIONS FOR A SINGLE LAYER

A thin layer having the thickness of H is laterally spread to infinity and its top and bottom surfaces are denoted by 1 and 2, respectively. The layer has a cylindrical hole into which a circular plate, namely, a sliced portion of the foundation is inserted. In addition, the layer is divided into an annular inner zone I and its surrounding outer zone o, as shown in Fig. 2. Owing to an approximate analysis, assume that the displacement linearly varies along the z-axis, and the vertical displacement during horizontal excitation and the horizontal one during vertical excitation are disregarded as like as discussed by Ikeda et al. (1992).

Now, let the circular plate translate horizontally in the x-direction with the displacement vector $\underline{U}_x = [U_{x1}, U_{x2}]^T$ with respect to the

faces (1, 2). In the above and following, the time function $e^{i\omega t}$ is omitted.
Denoting $\underline{U}_x$ in the cylindrical coordinates,

$$\underline{U}_x = \underline{u}_r \cos\theta - \underline{u}_\theta \sin\theta \qquad (1)$$

Then, the response displacement vectors ($\underline{u}_r^\Gamma$, $\underline{u}_\theta^\Gamma$) and stress vectors ($\underline{\sigma}_{rr}^\Gamma$, $\underline{\sigma}_{r\theta}^\Gamma$) of the surrounding soil in the Γ-zone (Γ = I or o) have the forms of

$$\underline{u}_r^\Gamma = \underline{v}_r^\Gamma \cos\theta \ , \qquad \underline{\sigma}_{rr}^\Gamma = \underline{p}_r^\Gamma \cos\theta$$
$$\underline{u}_\theta^\Gamma = \underline{v}_\theta^\Gamma \sin\theta \ , \qquad \underline{\sigma}_{r\theta}^\Gamma = \underline{p}_\theta^\Gamma \sin\theta \qquad (2)$$

Furthermore, the displacement and stress vectors represented by $\underline{v} = [\underline{v}_r^\Gamma, \underline{v}_\theta^\Gamma]^T$ and $\underline{p}^\Gamma = [\underline{p}_r^\Gamma, \underline{p}_\theta^\Gamma]^T$ satisfy the wave equation and can be written as

$$\underline{y}^\Gamma = \underline{S}^\Gamma \cdot \underline{A}^\Gamma \cdot \underline{Q}^\Gamma \quad (\Gamma = I, o) \qquad (3)$$

where

$\underline{y}^\Gamma$ = Displacement and stress vector,

$\underline{S}^\Gamma$ = Modal matrix of horizontal displacements of faces (1, 2),

$\underline{A}^\Gamma$ = Matrix relating to the lateral propagation of waves,

$\underline{Q}^\Gamma$ = Normal coordinates vector associated with modal matrix.

Omitting the superscript symbol of zone Γ, the above vectors $\underline{Y}$ and matrix $\underline{Q}$ are given by

$$\underline{Y} = [\underline{v}, \underline{p}]^T \qquad (4)$$
$$\underline{v} = [\underline{v}_r, \underline{v}_\theta]^T, \qquad \underline{p} = [\underline{p}_r, \underline{p}_\theta]^T$$
$$\underline{v}_r = [v_{r1}, v_{r2}]^T, \qquad \underline{p}_r = [p_{r1}, p_{r2}]^T$$
$$\underline{v}_\theta = [v_{\theta 1}, v_{\theta 2}]^T, \qquad \underline{p}_\theta = [p_{\theta 1}, p_{\theta 2}]^T$$

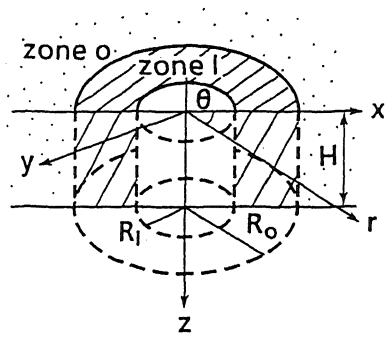

Figure 2. Single layer having a circular hole with annular inner and outer zones.

$$\underline{Q} = [\underline{q}, \underline{q}']^T \qquad (5)$$
$$\underline{q} = [\underline{q}_\alpha, \underline{q}_\beta]^T, \qquad \underline{q}' = [\underline{q}'_\alpha, \underline{q}'_\beta]^T$$
$$\underline{q}_\alpha = [q_{\alpha 1}, q_{\alpha 2}]^T, \quad \underline{q}'_\alpha = [q'_{\alpha 1}, q'_{\alpha 2}]^T$$
$$\underline{q}_\beta = [q_{\beta 1}, q_{\beta 2}]^T, \quad \underline{q}'_\beta = [q'_{\beta 1}, q'_{\beta 2}]^T$$

where

$\underline{q}$ = Normal coordinates vector of waves propagating in a positive r-direction,

$\underline{q}'$ = Normal coordinates vector of waves propagating in a negative r-direction,

$\underline{q}_\alpha$, $\underline{q}'_\alpha$ = Normal coordinates vectors relating to compressive waves,

$\underline{q}_\beta$, $\underline{q}'_\beta$ = Normal coordinates vectors relating to shear waves.

Furthermore, $\underline{S}$ and $\underline{A}$ are

$$\underline{S} = \begin{bmatrix} \underline{S}_{11} & \underline{S}_{22} \end{bmatrix} \qquad \underline{S}_{11} = \begin{bmatrix} [S] & \\ & [S] \end{bmatrix}$$
$$\underline{S}_{22} = \begin{bmatrix} [e_1][S] & \\ & [e_1][S] \end{bmatrix}, \quad [e_1] = \frac{1}{6}\begin{bmatrix} 2 & 1 \\ 1 & 2 \end{bmatrix} \qquad (6)$$

$$\underline{A} = \begin{bmatrix} -\frac{1}{2}\underline{B}_1(\alpha_\ell r) & \frac{1}{2}\underline{B}_2(\beta_\ell r) & -\frac{1}{2}\underline{B}'_1(\alpha_\ell r) & \frac{1}{2}\underline{B}'_2(\beta_\ell r) \\ \frac{1}{2}\underline{B}_2(\alpha_\ell r) & -\frac{1}{2}\underline{B}_1(\beta_\ell r) & \frac{1}{2}\underline{B}'_2(\alpha_\ell r) & -\frac{1}{2}\underline{B}'_1(\beta_\ell r) \\ \frac{GH}{r}\underline{C}_1(\alpha_\ell r) & \frac{GH}{r}\underline{C}_2(\beta_\ell r) & \frac{GH}{r}\underline{C}'_1(\alpha_\ell r) & \frac{GH}{r}\underline{C}'_2(\beta_\ell r) \\ \frac{GH}{r}\underline{C}_2(\alpha_\ell r) & \frac{GH}{r}\underline{C}_3(\beta_\ell r) & \frac{GH}{r}\underline{C}'_2(\alpha_\ell r) & \frac{GH}{r}\underline{C}'_3(\beta_\ell r) \end{bmatrix} \qquad (7)$$

$$\underline{B}(\ell)=\begin{bmatrix} B(1) & \\ & B(2) \end{bmatrix}, \quad \underline{C}(\ell)=\begin{bmatrix} C(1) & \\ & C(2) \end{bmatrix}$$

$$B_1(z) = \frac{dH_1^{(2)}(z)}{dz}, \quad B_2(z)= \frac{H_1^{(2)}(z)}{z}$$

$$B_1'(z) = \frac{dH_1^{(1)}(z)}{dz}, \quad B_2'(z)= \frac{H_1^{(1)}(z)}{z}$$

$$C_1(z) = 2H_2^{(2)}(z) - \frac{1}{\zeta^2} zH_1^{(2)}(z)$$

$$C_1'(z) = 2H_2^{(1)}(z) - \frac{1}{\zeta^2} zH_1^{(1)}(z)$$

$$C_2(z) = 2H_2^{(2)}(z), \quad C_2'(z) = 2H_2^{(1)}(z)$$

$$C_3(z) = 2H_2^{(2)}(z)-zH_1^{(2)}(z)$$

$$C_3'(z) = 2H_2^{(1)}(z)-zH_1^{(1)}(z)$$

$\zeta^{\Gamma} = V_s^{\Gamma} / V_p^{\Gamma}$.

V_s^{Γ} = Shear wave velocity.

V_p^{Γ} = Compressive wave velocity.

$H_\nu^{(1)}(z)$ = Hankel function of the 1st kind of the ν-th order.

$H_\nu^{(2)}(z)$ = Hankel function of the 2nd kind of the ν-th order.

In the above, α_ℓ^{Γ} and $\beta_\ell^{\Gamma}(\ell=1,2)$ and $\underline{S} = [\underline{X}_1, \underline{X}_2] = [\underline{Y}_1, \underline{Y}_2]$ satisfy the following eigen equations:

$$\begin{aligned} (\alpha^2[A_p]+[G_s]-\omega^2[M])\{X\} &= \{0\} \\ (\beta^2[A_s]+[G_s]-\omega^2[M])\{Y\} &= \{0\} \end{aligned} \tag{8}$$

where,

$$[A_s] = GH[e_1], \quad [G_s] = \frac{G}{H}[e_2]$$

$$[A_p] = (\lambda+2G)H[e_1], \quad [M]=\rho H[e_1]$$

$$[e_2] = \begin{bmatrix} 1 & -1 \\ -1 & 1 \end{bmatrix}$$

G^{Γ} :Shear modulus, λ^{Γ} :Lame's constant, ρ^{Γ} :Mass density.

It follows that

$$\begin{aligned} \alpha_1^{\Gamma} &= \zeta^{\Gamma}\beta_1^{\Gamma}, & \underline{X}_1^{\Gamma} &= [1,\ 1]^T \\ \alpha_2^{\Gamma} &= \zeta^{\Gamma}\beta_2^{\Gamma}, & \underline{X}_2^{\Gamma} &= [1,-1]^T \\ \beta_1^{\Gamma} &= \frac{1}{H}\frac{\omega H}{V_s^{\Gamma}}, & \underline{Y}_1^{\Gamma} &= [1,\ 1]^T \\ \beta_2^{\Gamma} &= -i\frac{1}{H}[12-(\omega H/V_s^{\Gamma})^2]^{1/2}, & \underline{Y}_2^{\Gamma} &= [1,-1]^T \end{aligned} \tag{9}$$

Evidently, the stresses and displacements in the I and o zones satisfy the condition of continuity at $r=R_o$

$$\underline{V}^I(R_o) = \underline{V}^o(R_o) \tag{10}$$

where,

$$\underline{V}^I(R_o)=\underline{S}\cdot\underline{A}^I(R_o)\cdot\underline{Q}^I, \quad \underline{V}^o(R_o)=\underline{S}\cdot\underline{A}^o(R_o)\cdot\underline{Q}^o$$

It connects the normal coordinates vector of the inner zone $\underline{Q}^I$ with that of the outer zone $\underline{Q}^o$ as

$$\underline{Q}^I = [\underline{A}^I(R_o)]^{-1}\cdot\underline{A}^o(R_o)\cdot\underline{Q}^o \tag{11}$$

Furthermore, the displacements and stresses of the inner zone $\underline{V}^I(R_I)$ can be written in terms of the normal coordinates of the outer zone $\underline{Q}^o$:

$$\underline{V}^I(R_I)=\underline{S}\cdot\underline{A}^I(R_I)\cdot[\underline{A}^I(R_o)]^{-1}\cdot\underline{A}^o(R_o)\cdot\underline{Q}^o \tag{12}$$

In particular, one has $(\underline{q}')^{\Gamma} = \{0\}$ in the outer zone, so that Eq.(12) can be separated into the equation of displacement vector and that of force vector:

$$\underline{v}^I(R_I) = \underline{S}_{11}\cdot\underline{D}\cdot\underline{q}^o, \quad \underline{D} = [\underline{D}_{jk}] \tag{13}$$

$$\underline{D}_{jk}=\begin{bmatrix} D_{jk}^1 & \\ & D_{jk}^2 \end{bmatrix}, \quad (j,k)=(1,2)$$

$$\underline{p}^I(R_I) = \underline{S}_{22}\cdot\underline{E}\cdot\underline{q}^o, \quad \underline{E} = [\underline{E}_{jk}] \tag{14}$$

$$\underline{E}_{jk}=\begin{bmatrix} E_{jk}^1 & \\ & E_{jk}^2 \end{bmatrix}, \quad (j,k)=(1,2)$$

Since the cylindrical hole in the inner zone maintains its circular shape, one has

$$\underline{v}_r^I(R_I) + \underline{v}_\theta^I(R_I) = \{0\}$$

Hence, Eq. (13) leads to

$$\underline{q}^{o}_{\beta} = -(\underline{D}_{12}+\underline{D}_{22})^{-1}(\underline{D}_{11}+\underline{D}_{21})\cdot\underline{q}^{o}_{\alpha} = \underline{J}\cdot\underline{q}^{o}_{\alpha} \quad (15)$$

Thus, the displacement along the x-direction of the hole surface $\underline{U}_x$ is represented by the following form:

$$\underline{U}_x = [S](\underline{D}_{11}+\underline{D}_{12}\cdot\underline{J})\cdot\underline{q}^{o}_{\alpha} \quad (16)$$

Likewise, using Eqs. (14), (15) and (16), the resultant force on the hole surface in the x-direction as a whole is obtained as

$$\begin{aligned}\underline{P}_x &= \pi R_I(\underline{p}_r - \underline{p}_\theta)\\ &= \frac{\pi R_I}{2}[e_1][S](\underline{E}_{11}-\underline{E}_{21}+(\underline{E}_{12}-\underline{E}_{22})\cdot\underline{J})\\ &\quad\cdot(\underline{D}_{11}+\underline{D}_{12}\cdot\underline{J})^{-1}[S]\,\underline{U}_x \end{aligned} \quad (17)$$

Eq. (17) can be rewritten in such a form as defining the laterally axial stiffness k_a and the shear stiffness k_b,

$$\underline{P}_x = \underline{k}\cdot\underline{U}_x \quad (18)$$

$$\underline{k} = \frac{k_a}{2}\begin{bmatrix}1 & 0\\ 0 & 1\end{bmatrix} + k_b\begin{bmatrix}1 & -1\\ -1 & 1\end{bmatrix}$$

When the layers are stratified over the embedment depth D, the shear stiffness of the individual j-th layer of the thickness H_j requires the multiplication of D/H_j to k_b in Eq. (18) for a single layer, because of its series connection.

Next, as a case of vertical excitation, let the circular rigid plate rotate around the y-axis. Then, the SV-wave alone propagates in the single layer. Noticing that the present case takes the scalars of displacement and stress because of their uniform distribution across the thickness, the response of the surrounding soil may be expressed in a manner as like as Eq. (2),

$$u_z^{\Gamma} = v_z^{\Gamma}\cos\theta \ , \quad \sigma_{rz}^{\Gamma} = p_z^{\Gamma}\cos\theta \quad (19)$$

Corresponding to Eq. (3), one can write

$$\underline{v}^{\Gamma} = \underline{B}^{\Gamma}\cdot\underline{q}^{\Gamma} \quad (20)$$

where

$$\underline{v}^{\Gamma} = [v_z^{\Gamma}, p_z^{\Gamma}]^T, \quad \underline{q}^{\Gamma} = [q^{\Gamma}, (q')^{\Gamma}]^T$$

$$\underline{B}^{\Gamma} = \begin{bmatrix}B_{11}^{\Gamma} & B_{12}^{\Gamma}\\ B_{21}^{\Gamma} & B_{22}^{\Gamma}\end{bmatrix}, \quad \beta^{\Gamma} = \frac{1}{\bar{H}}\frac{\omega H}{V_s^{\Gamma}}$$

$$B_{11}^{\Gamma} = H_1^{(2)}(\beta^{\Gamma} r), \quad B_{12}^{\Gamma} = H_1^{(1)}(\beta^{\Gamma} r)$$

$$B_{21}^{\Gamma} = -G^{\Gamma} H\beta^{\Gamma}\frac{dH_1^{(2)}(\beta^{\Gamma} r)}{d(\beta^{\Gamma} r)} \quad (21)$$

$$B_{22}^{\Gamma} = -G^{\Gamma} H\beta^{\Gamma}\frac{dH_1^{(1)}(\beta^{\Gamma} r)}{d(\beta^{\Gamma} r)}$$

$$\begin{aligned} v_z &= [B_{11}^{I}(R_I)\ B_{12}^{I}(R_I)]\cdot[\underline{B}^{I}(R_o)]^{-1}\begin{bmatrix}B_{11}^{o}(R_o)\\ B_{21}^{o}(R_o)\end{bmatrix} q^{o}\\ &= F_v\, q^{o}\end{aligned}$$

$$\begin{aligned} p_z &= [B_{21}^{I}(R_I)\ B_{22}^{I}(R_I)]\cdot[\underline{B}^{I}(R_o)]^{-1}\begin{bmatrix}B_{11}^{o}(R_o)\\ B_{21}^{o}(R_o)\end{bmatrix} q^{o}\\ &= F_p\, q^{o}\end{aligned}$$

As a result, the rotational stiffness k_c can be obtained as

$$M_y = \pi R_I^2\, p_z(R_I) = k_c\Theta \quad (22)$$

$$k_c = \pi R_I^3\,\frac{F_p}{F_v}$$

3 SIMULATION ANALYSIS OF THE FORCED VIBRATION TEST OF REINFORCED CONCRETE BLOCK

The specimen was a reinforced concrete block of 4m x 4m x 6mH of Mizuno et al. (1985). The test was carried out for two soil conditions (A) and (B), as shown in Fig. 3(i). These correspond to the pre- and post- embedment to investigate the influence of backfill soil. The physical properties of the soil have been estimated by the field survey and laboratory test. In the case (A) of neglecting the existence of the surface layer of 2m thick, the block is directly supported on the bottom soil which is assumed as a uniform halfspace having the shear wave velocity of V_s=440m/s.

In the case (B), the block rests on the bottom soil and laterally backfilled by the soft soil which has V_s=150m/s for its upper part of 1m thick and V_s=190m/s for the remaining. These backfilled soil are laterally surrounded by the surface layer of V_s=420m/s.

The experimental and analytical results are compared as shown in Figs. 3(i) and 3(ii), respectively. The curves are drawn for the frequency response functions of the horizontal displacement amplitude at the center of

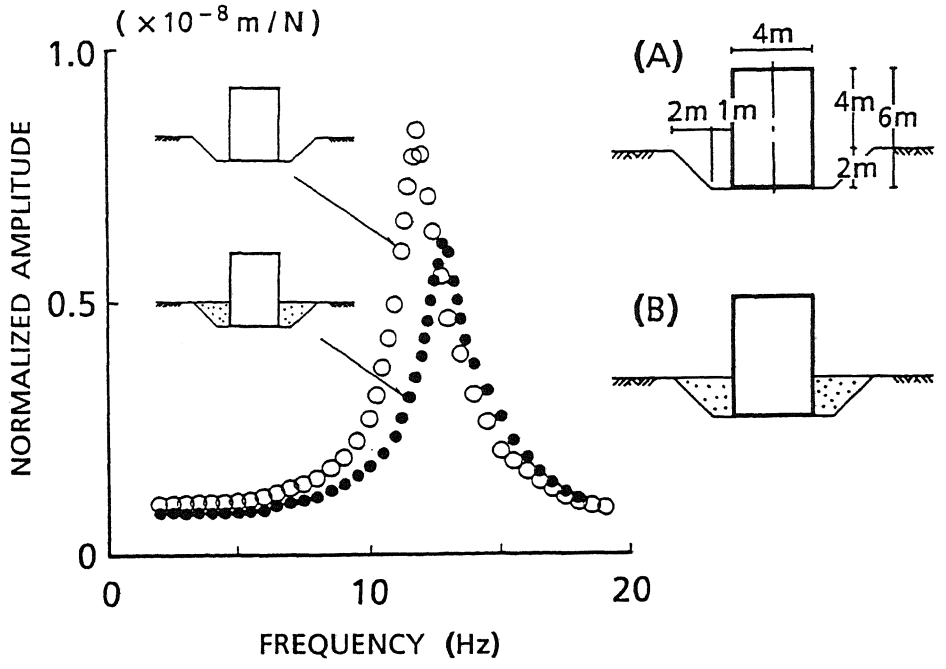

(i) Test results

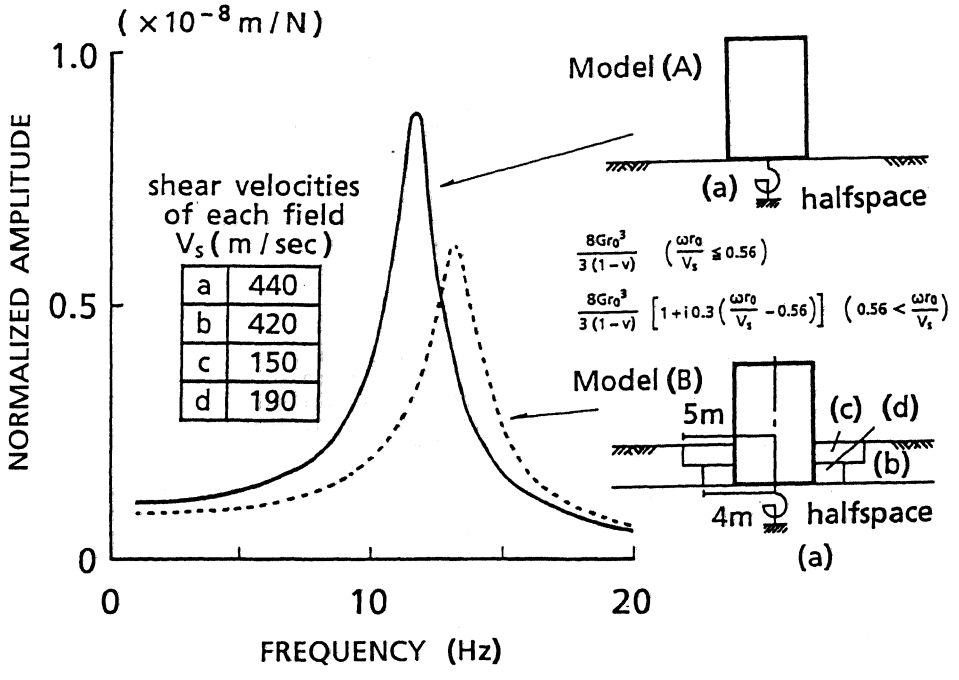

(ii) Analysis results

Figure 3. Plots of amplitude of horizontal displacement at the center of gravity versus frequency comparing the test result to analysis result.

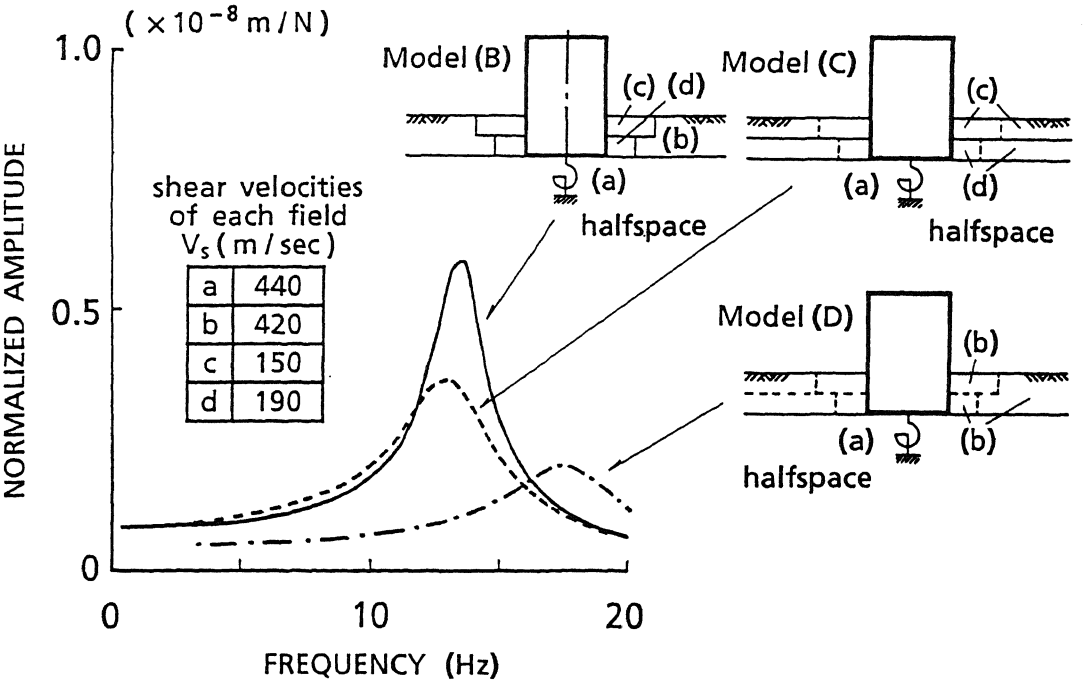

Figure 4. Plots of amplitude of horizontal displacement at the center of gravity versus frequency in comparing the analysis results due to three kinds of Model (B), (C) and (D).

gravity of the block. From the figures, it is found that simulation analysis predicts well the resonant frequencies and associated amplitudes being in close agreement with the experimental results in both cases.

The supplemental analysis is performed to investigate the effect of the lateral boundary of the backfill soil by using two models of (C) and (D), as shown in Fig. 4. The model (C) has the backfill soil as same as used for the model (B) and unbounded, while the model (D) has no backfill and is directly surrounded by the surface layer of V_s=420m/s. As a result, the model (C) indicates that the resonant frequency decreases slightly and the resonant amplitude becomes as low as 60% of the results of the experiment. On the other hand, the model (D) indicates that the resonant frequency shifts toward the higher range and the associated amplitude becomes about 1/3 of the experimental results. From these findings, it is found that as far as concerned to the present configuration of the model, (1) the resonant frequency mainly depends on the rigidity of soil of the inner zone and (2) the radiation damping decreases owing to the reflection of waves from the boundary with the surrounding hard soil

4 CONCLUSIONS

In order to predict the dynamic characteristics of a structure embedded and surroundingly backfilled, the present paper proposes a practical method of obtaining the foundation stiffness relating to the embedment in a radially inhomogeneous soil. The availability of the method is verified by performing the simulation analysis to the field test of forced vibration of a reinforced concrete block. Probably, the method will be applicable to deal with the nonlinearity of soil surrounding embedded structures.

REFERENCES

Ikeda, Y., Shimomura, Y. & Tajimi, H. 1992. A simplified method of obtaining interaction stiffnesses associated with the embedment of structures. to be presented to 10WCEE.

Mizuno, N. et al. 1985. Verification of aseismic design by using experimental results. Transactions of The 8th SMiRT. Vol.K(a): 293-298.

Novak, M. & Sheta, M. 1980. Approximate approach to contact effects of piles. Special Technical Publication on Dynamic Response of Pile Foundations ; Analytical Aspects, ASCE: 53-79.

Veletsos, A.S. & Dotson, K.W. 1988. Horizontal impedance for radially inhomogeneous visco-elastic layers. Earthquake Engineering & Structural Dynamics. Vol.16: 947-966.